EVOLUTIONARY BIOLOGY

Blue reflectance in tarantulas is evolutionarily conserved despite nanostructural diversity

Bor-Kai Hsiung,[1]* Dimitri D. Deheyn,[2] Matthew D. Shawkey,[1] Todd A. Blackledge[1]

Slight shifts in arrangement within biological photonic nanostructures can produce large color differences, and sexual selection often leads to high color diversity in clades with structural colors. We use phylogenetic reconstruction, electron microscopy, spectrophotometry, and optical modeling to show an opposing pattern of nanostructural diversification accompanied by unusual conservation of blue color in tarantulas (Araneae: Theraphosidae). In contrast to other clades, blue coloration in phylogenetically distant tarantulas peaks within a narrow 20-nm region around 450 nm. Both quasi-ordered and multilayer nanostructures found in different tarantulas produce this blue color. Thus, even within monophyletic lineages, tarantulas have evolved strikingly similar blue coloration through divergent mechanisms. The poor color perception and lack of conspicuous display during courtship of tarantulas argue that these colors are not sexually selected. Therefore, our data contrast with sexual selection that typically produces a diverse array of colors with a single structural mechanism by showing that natural selection on structural color in tarantulas resulted in convergence on similar color through diverse structural mechanisms.

INTRODUCTION

Colors of living organisms are produced by selective absorption of certain wavelengths of light by pigments, by light scattering from nanostructures, or by the interaction of these two mechanisms (1, 2). Nanostructures produce color through various physical mechanisms including diffraction, coherent scattering, and interference (3). These colors, and the nanostructures that produce them, evolve mostly through complex interactions between sexual and natural selection for visual function.

Sexual selection is typically predicted to increase color and pattern diversity between closely related populations (4, 5). In turn, high color diversity caused by sexual isolation through mating preferences may increase speciation rates (6) [but see the study by Irestedt et al. (7)]. Natural selection, on the other hand, often homogenizes color and pattern in species where they share common function in similar habitats. For example, aposematic species benefit from Müllerian mimicry, whereas cryptic species often show similar background color matching or outline disruption (8). Moreover, color can also perform nonsignaling functions such as thermoregulation (9). Iridescent colors may even evolve as a by-product of structures functioning in abrasion resistance (10), mechanical strengthening (11), and locomotion (12). Thus, distinguishing between the effects of sexual selection and natural selection and how they affect colors and color patterns in natural populations can be challenging. Therefore, studying color in a group of animals with limited visual capacities provides a unique opportunity to investigate how color evolves through natural selection without the confounding influence of sexual selection.

Tarantulas (Araneae: Theraphosidae) are one of the most basal groups of spiders and are contained within the Mygalomorphae, which diversified from most other spiders almost 300 million years ago (Ma) (13). Theraphosidae now consists of 112 genera (version 15.0, July 2014, N. I. Platnick, http://research.amnh.org/iz/spiders/catalog_15.0/). Ta-

rantulas are largely nocturnal ambush predators that reside in retreats or burrows (14) and primarily navigate by chemotactile senses (15). Although tarantulas have eight eyes, like most other spiders, their visual ability is highly limited because they only have a single type of photopigment and have low acuity (16). Despite their poor vision, many tarantula species show vibrant blue coloration (Fig. 1 and fig. S1). Although previous work revealed that these colors are structural in origin and likely produced via multilayer interference effects (17, 18), the evolutionary diversification of both the nanostructures and the colors they produced has not been addressed. By using an integrative approach, combining reflectance spectroscopy, electron microscopy, and theoretical modeling, we here examine the evolution of coloration in the absence of intraspecific visual color signaling using tarantulas as a model system.

RESULTS

Blue coloration is common in tarantulas whereas green coloration is rare

We surveyed the colors of tarantulas from 53 genera, covering 7 of 10 subfamilies of Theraphosidae and mapped color onto a phylogenetic supertree (fig. S2). At least one species in all tarantula genera had colors typically produced by pigments (yellow, orange, red, brown, and black). A total of 40 of 53 genera also had blue coloration, including all seven subfamilies (fig. S2, blue). Only 12 genera showed green coloration, and almost half of them (5 of 12) were in the subfamilies of Aviculariinae and Stromatopelminae. Blue is thus a common color in tarantulas, whereas green is conspicuously rarer. To reconstruct color evolution, we used a conservative approach by assuming that blue was the ancestral color for any genus containing at least one blue species (it is often likely a derived trait within a few species in many of these genera). On the basis of this assumption, blue evolved at least eight times in tarantulas (Fig. 1), although the actual number of origins is likely greater.

Blue hairs result from diverse structures in different species

We used both scanning electron microscopy (SEM) and transmission electron microscopy (TEM) to investigate the mechanistic basis of the

[1]Department of Biology and Integrated Bioscience Program, The University of Akron, Akron, OH 44325–3908, USA. [2]Scripps Institution of Oceanography, University of California, San Diego, La Jolla, CA 92093, USA.
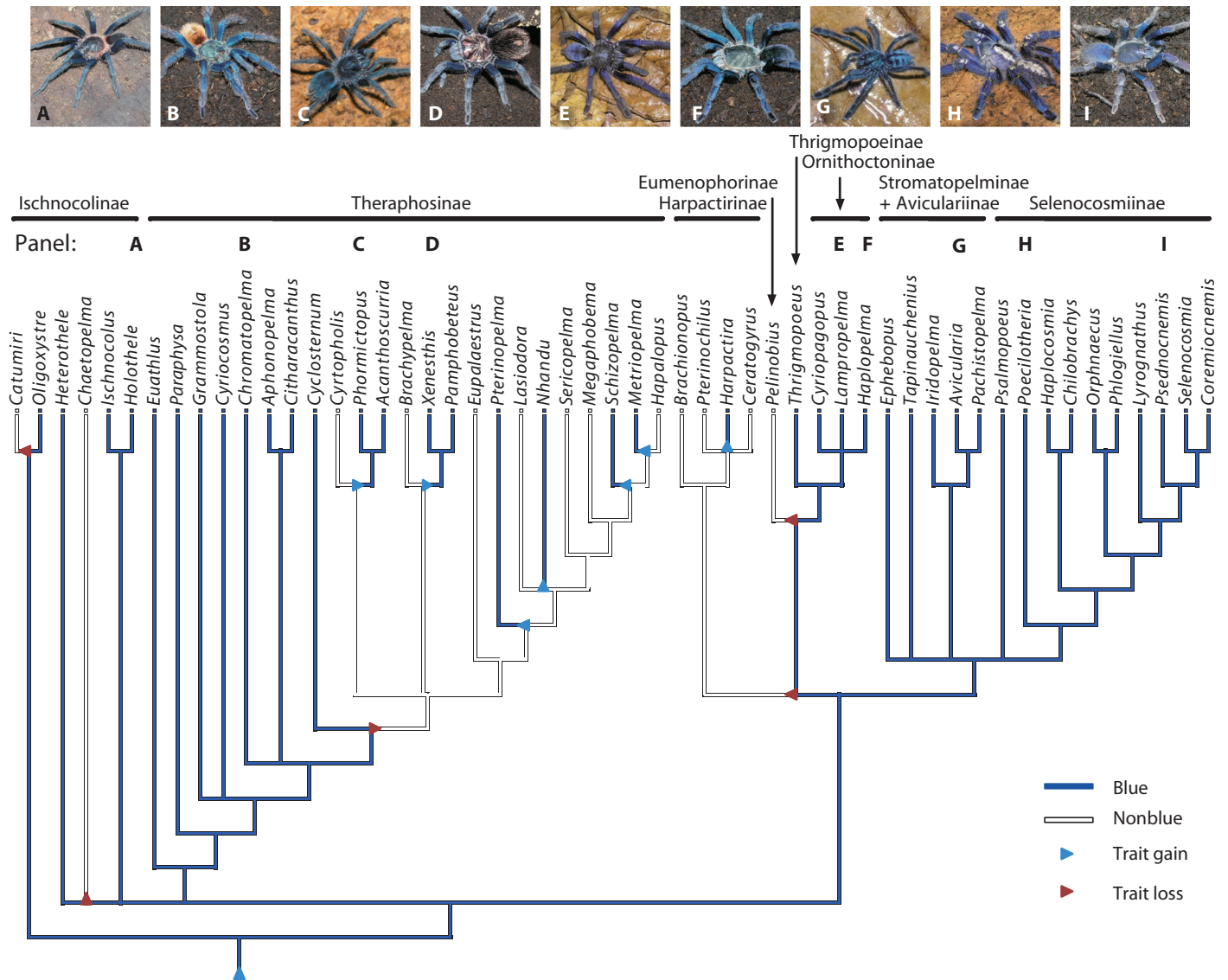*Corresponding author. E-mail: bh63@zips.uakron.edu

Fig. 1. Ancestral character analysis for blue coloration. Blue color evolved at least eight times (▲) and was lost at least five times (▲) during evolution of Theraphosidae. The basal origin of blue is likely an artifact to the highly conservative assignment of blue as the ancestral state for any genus containing a blue species. (**A** to **I**) Photos representing the appearance of nine blue tarantula species are shown above the phylogeny. Photos courtesy of T. Patterson.

blue color in specialized hairs. At least three different morphologies were found under SEM: (i) smooth, rod-shaped hairs (Fig. 2, A and H); (ii) symmetric hairs with an array of rodlike, tubular foldings projecting longitudinally on their periphery (Fig. 2, D and G); and (iii) asymmetric hairs with longitudinal, bladelike protrusions on one or more sides (Fig. 2, B, C, and E) or irregularly flattened hairs (Fig. 2F). Nanostructures were present immediately beneath the cortex of the hairs for all species except *G. rosea* (Fig. 3, column I) and were either (i) quasi-ordered spongy structures (Fig. 3, A to C) or (ii) more organized multilayered structures (Fig. 3, D to G). Multilayers within asymmetric, platelike protrusions of the blue hairs on the chelicerae of *E. cyanognathus* had been reported previously by Foelix *et al.* (18). The nanostructures were composed of two alternating materials with high and low electron densities in TEM micrographs (Figs. 2 and 3). According to previous reports, the high–electron density material is a chitin-protein

composite and the low-density material is air (17, 18). We verified this by a refractive index (n_r) matching test, in which color disappeared when hairs were submerged in quinoline liquid (n_r = 1.63) (fig. S3). This also suggests that the n_r for the chitin-protein composite material in tarantulas is about 1.63 and is thus consistent with published estimates (17).

Highly conserved blue spectrum is observed across species

Reflectance spectra of single blue hairs from different tarantulas were measured by microspectrophotometry (Fig. 2). The reflectance peaks of those blue hairs were closely distributed around 450 nm (Fig. 4A). For comparison, we compiled data on blue colors of *Polyommatus* butterflies (19) and found that they are distributed across a much broader range of blues (Fig. 4B). We then compiled data to include all species of blue Lepidoptera (butterflies and moths) and Aves (birds) with hue (measured as wavelength of peak reflectance) available in the
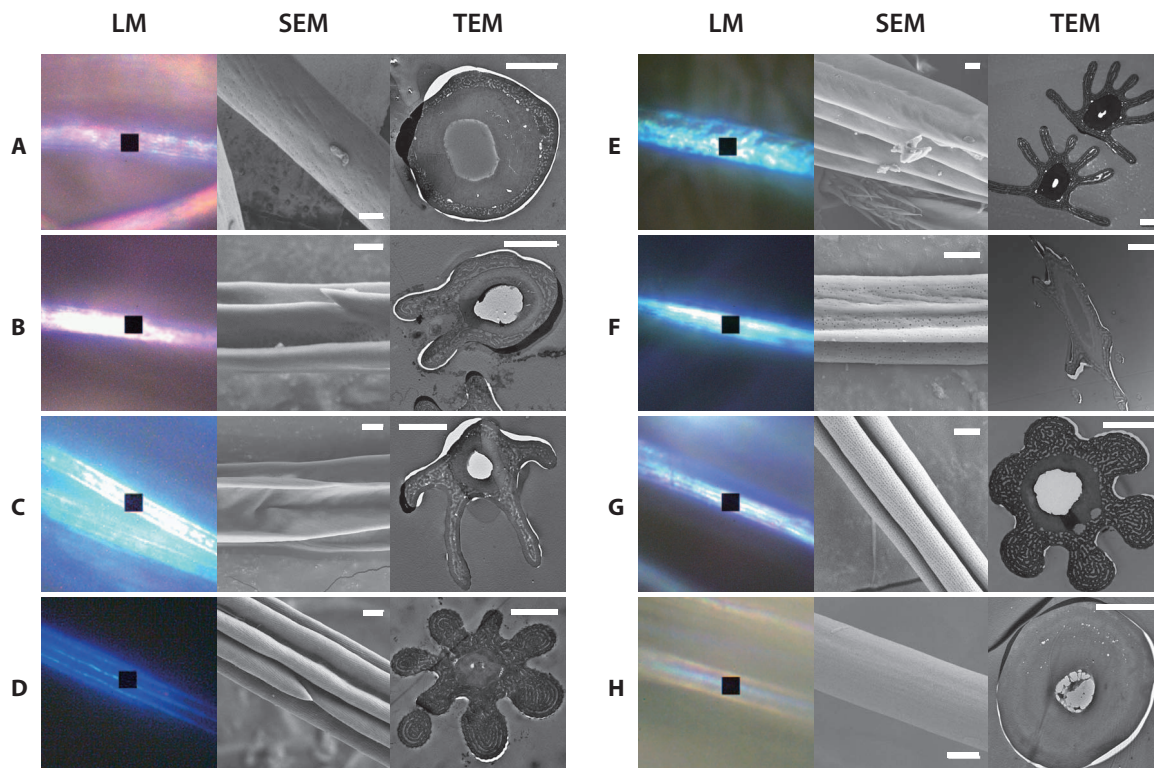
LM   SEM   TEM   LM   SEM   TEM

Fig. 2. Color, morphology, and nanostructure of blue hairs. Colors observed under a microspectrophotometer [light microscopy (LM)]. Center black square (spectra-measured area), 4 × 4 μm. (**A** to **H**) Three types of hair morphology were observed under SEM: (i) smooth cylindrical hairs (A and H), (ii) irregular/bladelike protruding hairs (B, C, E, and F), and (iii) symmetric lobe-like protruding hairs (D and G). Two types of nanostructures were observed under TEM: (i) multilayer structure (D to G) and (ii) quasi-ordered structure (A to C). High-reflectance ridges are observed in (D). The center portion of the hair in (H) is blue, but not on the periphery. This is probably caused solely by the optical effect of a hollow, semitransparent fiber (that is, the hair). No conspicuous nanostructure was observed in (H). Scale bar, 2 μm. (A) *Euathlus pulcherrimaklaasi*. (B) *Tapinauchenius violaceus*. (C) *Chromatopelma cyaneopubescens*. (D) *Lampropelma violaceopes*. (E) *Ephebopus cyanognathus* (TEM photo courtesy of R. F. Foelix). (F) *Avicularia laeta*. (G) *Poecilotheria metallica*. (H) *Grammostola rosea*.

published literature. We focused on hue because its value is usually consistent across different instruments, radiometric light sources, and spectral alignment and calibration techniques (table S1). The peak distribution for Theraphosidae [mean ± SD, 450 ± 21 nm; coefficient of variation (c.v.), 4.65%] was narrower than that for clades with visually conspicuous mating rituals—Lepidoptera (mean ± SD, 454 ± 41 nm; c.v., 8.94%) and Aves (mean ± SD, 434 ± 27 nm; c.v., 6.13%) (Fig. 5A and table S1). The absolute distance of each species' peak reflectance from the average was significantly different when comparing Theraphosidae to Lepidoptera ($P = 0.039$) but not to Aves ($P = 0.264$) under Mann-Whitney U tests (Fig. 5B). However, when the single statistical outlier in Theraphosidae is removed, the difference of peak distribution between Theraphosidae and Aves becomes more evident, but remains not statistically significant ($P = 0.084$), potentially because of the small sample size.

Theoretical modeling verified the structural basis of blue

We calculated theoretical reflectance spectra using the Fourier Analysis Tool for Biological Nano-optics (20). Peak reflectance, but not the overall shapes, of these theoretical spectra matched the measured spectra fairly well (Table 1) (Fig. 3, column III, and Fig. 4A), suggesting that these colors are produced by coherent scattering mechanisms. The lack of overall shape match is a known limitation for this type of analysis, and thus, this tool is most useful when distinguishing between

disordered and periodic structures with either crystal-like, multilayer, or quasi-ordered structure (21).

Calculated reflectance spectra for *L. violaceopes*, *E. cyanognathus*, *A. laeta*, and *P. metallica* based on multilayer interference are shown in Fig. 4A (dashed line), where the calculated spectrum of *P. metallica* agrees with the previously reported calculation by Foelix *et al.* (22). Theoretical and empirical spectra matched well, particularly for *L. violaceopes*. Some spectral shape deviations between measurements and calculations could be explained by complex surface morphologies of the hairs. Higher reflectance at longer wavelengths could be caused by nonspecific scattering, which is not taken into account in the multilayer interference model.

Structural colors produced by interference are mostly highly iridescent (3). However, blue colors observed in tarantulas were conspicuously angle-independent (fig. S4) to nonassisted human vision, even for blues from *L. violaceopes* and *P. metallica* where the colors were produced by multilayer interference. With that said, those hairs still show minor iridescence when observed under a microscope, similar to fig. S3A. This suggests that those hairs are indeed iridescent microscopically. However, the iridescent effect of those hairs is beyond the spatial resolution of normal human vision and hence is not detected.

Using both coherent scattering and multilayer interference models, we verified that quasi-ordered and multilayer structures are indeed the structural basis for the production of blue coloration in tarantulas
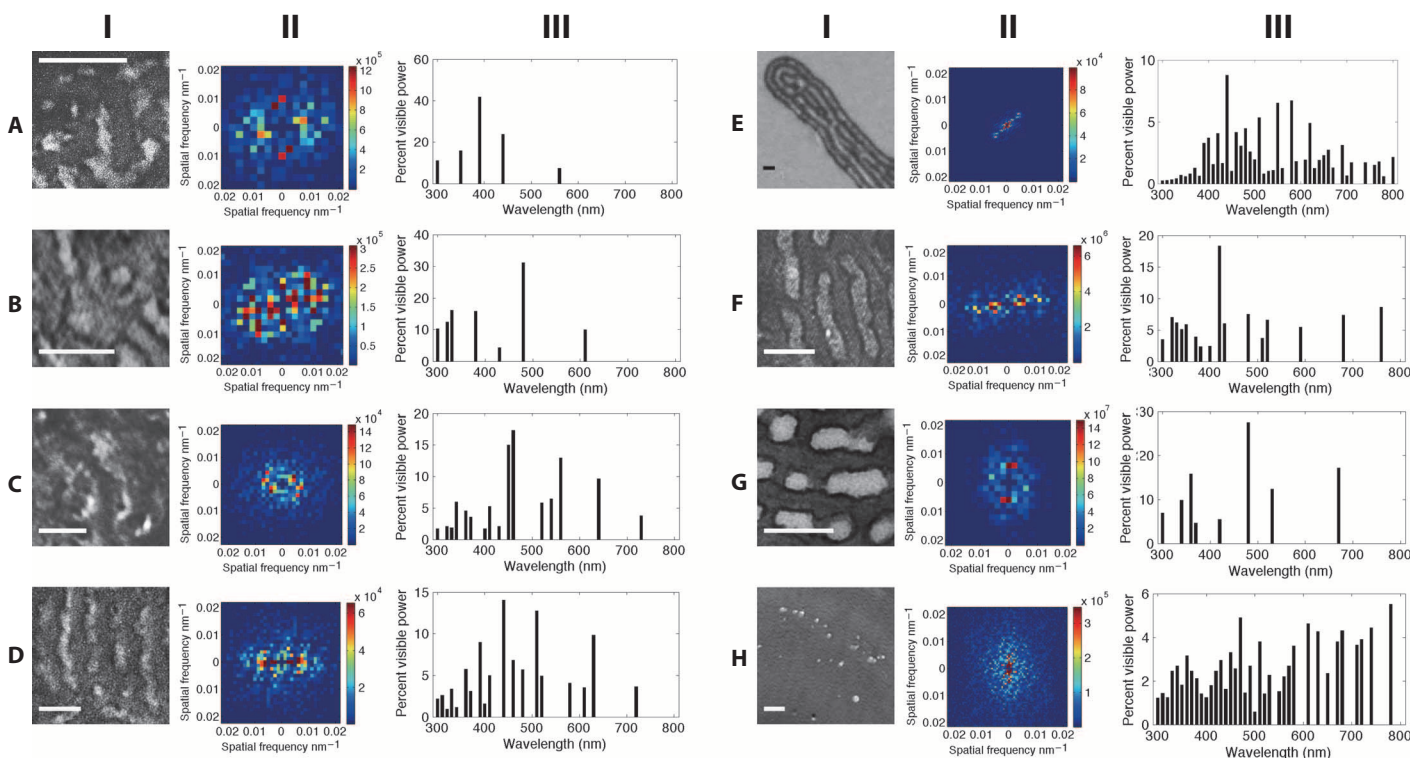
Fig. 3. Coherent scattering analyses by Fourier Analysis Tool for Biological Nano-optics. Column I: Selected TEM micrographs that represent observed nanostructures. (**A** to **H**) Quasi-ordered structure (A to C) and multilayer structure (D to G). No structure is seen in (H). Scale bar, 250 nm. Column II: Two-dimensional (2D) Fourier power spectra of column I. Column III: Predicted reflectance spectra based on column II. (A) *E. pulcherrimaklaasi*. (B) *T. violaceus*. (C) *C. cyaneopubescens*. (D) *L. violaceopes*. (E) *E. cyanognathus* (photo courtesy of R. F. Foelix). (F) *A. laeta*. (G) *P. metallica*. (H) *G. rosea*.

(Table 1). This is with the exception of *G. rosea*, whose color appears to be produced by a combination of optical effects between thin, hollow, semitransparent hairs and pigments.

DISCUSSION

Blue color evolved independently at least eight times in tarantulas. Remarkably, these colors converge within a narrow band of blue despite being produced by at least three different mechanisms: (i) multilayer lamina structures, (ii) quasi-ordered spongy structures, and (iii) no conspicuous nanostructure at a suitable scale for structural color production. The poor vision of tarantulas makes it unlikely that these colors serve as an intraspecific mating signal, and thus, our data illustrate how colors evolve in the absence of sexual selection.

Throughout living organisms, blues are almost always produced by structural mechanisms, ranging from quasi-ordered structures to 1D, 2D, and 3D photonic crystals (*23, 24*). Blue coloration in birds and insects is often produced by quasi-ordered or multilayered structures (that is, 1D photonic crystal), and we found that these two structural mechanisms also produce blue in tarantulas.

All of the structural mechanisms above are capable of producing a broad range of colors simply by altering their periodic spatial distances, without the need to change the overall structures or underlying materials (*25*), making these colors easy to diversify once the nanostructures evolve. As a result, structural colors can achieve a greater range of colors relative to pigmentary colors (*26*). Moreover, structural colors

have features that are often preferred in mating displays, such as increased brightness and high directional dependence (that is, iridescence) (*27*). Hence, novel structural color innovation can correlate with increased rates of speciation (*28*). However, blue colors in tarantulas show very little iridescence compared to sexually selected systems in birds and insects (fig. S4). This decreased iridescence may be caused by the complex morphology of the specialized blue hairs (Fig. 2), which attenuates the iridescence produced by the multilayer structure underneath the cortex of the hairs. In addition, the blue color in tarantulas is highly conserved, peaking within a narrow 20-nm band around 450 nm. These patterns are unlikely to be driven by sexual selection.

The monochromatic photoreceptors in tarantula eyes are most sensitive to light around 500 nm (*16*). This lack of overlap between wavelengths and photosensitivity, as well as the poor visual acuity of tarantulas and lack of noticeable visual courtship, argues that the blue coloration in tarantulas is not an intraspecific sexual signal but is instead the result of natural selection for some (to-be-identified) functions. Several lines of evidence reinforce that these blue colors are not sexual signals: (i) Tarantula eyes are simple ocelli located on the top of the carapace like other "nonvisual" spiders (*14*) and contrast with the much larger specialized image-forming eyes that lie on the front of the carapace in highly visual spiders, such as Salticidae (jumping spiders), Lycosidae (wolf spiders), Thomisidae (crab spiders), Sparassidae (huntsman spiders), and Deinopidae (gladiator spiders) (*29*). (ii) On the basis of electrophysiology and behavioral evidence, only jumping spiders (*30, 31*) and crab spiders (*32, 33*) are reported to have color vision, and only Salticidae widely use colors in courtship display [for example, the peacock
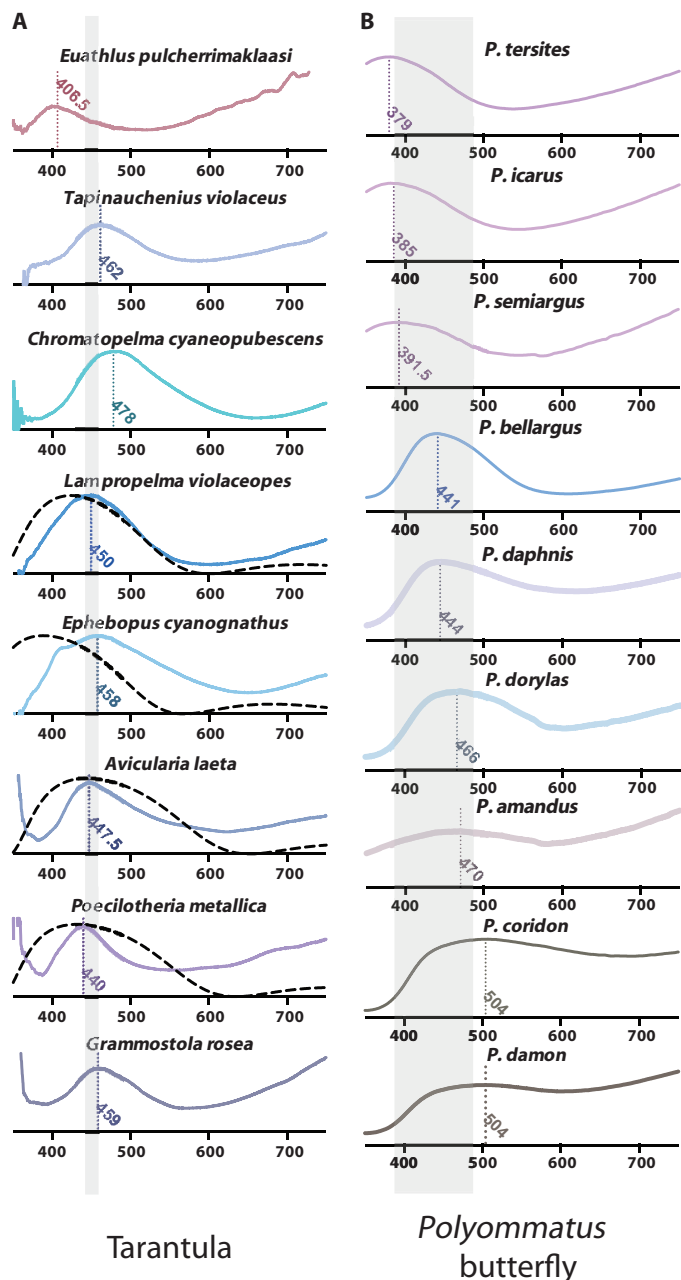
Fig. 4. Reflectance spectra of tarantulas and *Polyommatus* butterflies. (**A**) Normalized reflectance spectral measurements of tarantulas (solid lines) show conservation of peak reflectance around 450 nm. Theoretical spectra are calculated from multilayer simulations (dashed lines) and matched the measured spectra fairly well. (**B**) Normalized reflectance spectral measurements of *Polyommatus* butterflies (*19*) show peak reflectance broadly distributed across 400 to 500 nm. The gray area indicates the interquartile range.

Fig. 5. Distribution of blue colorations in Theraphosidae, Lepidoptera, and Aves. (**A**) Scatterplots (means ± SD) of reflectance peak positions for blue Theraphosidae, Lepidoptera, and Aves. Reflectance peak distribution in Theraphosidae has a trend to be narrower than that in Lepidoptera and Aves. The c.v. is 4.65% for Theraphosidae, 8.94% for Lepidoptera, and 6.13% for Aves. (**B**) Scatterplot for the data points in (A) and their differences to the mean value of each group. The smaller the value, the closer it resides to the mean. However, only Lepidoptera, not Aves, show a significant difference from Theraphosidae ($P = 0.039$), designated by the asterisk sign, potentially because of the outlier in Theraphosidae and the small sample size. Data for the Theraphosidae group are from our own observations, whereas those shown for the Lepidoptera and Aves groups are from data available from the literature. The Lepidoptera group is composed of nine species of *Polyommatus* butterflies from Fig. 4 and nine other species from table S1. The Aves group is composed of 10 species from table S1, including birds from three different orders: (i) parrot (Psittaciformes), (ii) penguin (Sphenisciformes), and (iii) songbird (Passeriformes).

trast, blue tarantulas often present colors as early, immature instars (*37*). Some even lose their blue coloration when molting to adulthood (for example, *A. laeta*). In addition, blue colors in tarantulas do not occur in regions that are easily seen when they engage in mating postures (that is, raising the front legs and prosoma), such as the underside of the front legs and cephalothorax. (iii) The courtship and mating behaviors of tarantulas lack conspicuous visual signals, regardless of color, and instead heavily depend on vibratory and chemical cues (*38*). Thus, the preponderance of evidence supports the hypothesis that tarantulas have poor vision and thus that sexual selection does not explain the evolution of their colors.

The conservation of blue color in tarantulas is even more remarkable when considering how rapidly structural colors can evolve. Although the tarantula (family: Theraphosidae), butterfly and moth (order: Lepidoptera), and bird (class: Aves) clades all emerged around the same geologic time (circa 100 Ma) (*13*, *39*, *40*), blue colors are distributed more broadly across the short-wavelength spectrum in Lepidoptera relative to Theraphosidae (Fig. 5). In particular, blue *Polyommatus* butterflies diversified less than 4 Ma (*41*), but their blue reflectance peaks are spread across the spectrum from the 400- to 500-nm range (Fig. 4B). In addition, an artificial selection experiment successfully shifted the reflectance peaks of butterflies 40 to 50 nm toward red after only six generations of selection in less than 1 year (*42*). The silver color produced by guanine crystals evolved independently from white at least eight times in Araneomorphae (*43*). Whether these shifts were driven by natural and/or sexual selection should be investigated in the future.

Despite underlying morphological diversity, conserved reflectance in a specific narrow band of wavelengths suggests a signaling function, but the receiver of that signal for tarantulas remains unclear. The natural

spiders (*Maratus* spp.)] (*34*). Although visual display is important for wolf spiders in courtship (*35*, *36*), it is likely that achromatic contrast, not hue, is involved in the visual display of lycosids because they lack conspicuous chromatic colors. Salticids are sexually dimorphic and the adult males typically have bright colors in body regions that are visible during courtship, such as the chelicerae, pedipalp, and front legs. In con-
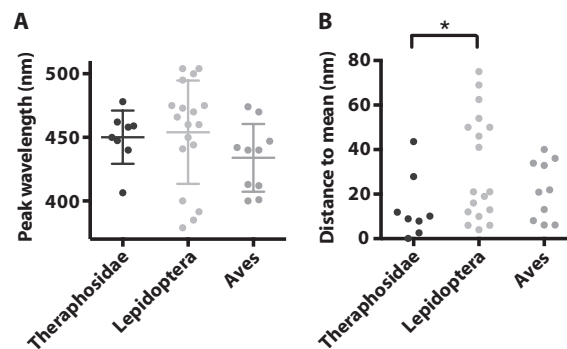
Table 1. Results summary. FFT, fast Fourier transform; ml, multilayer; n.a., not applicable.

Species	Condition	Color, region	Observed peak (nm)	Predicted peak (nm)	Hair nanostructure	Thickness/ distance (nm)	Native location
E. pulcherrimaklaasi	Subadult, dissecting	Purple, leg	406.5	390 (FFT)	Quasi-ordered	120.4*	Ecuador, ground habitat
T. violaceus	Subadult, dissecting	Purple, leg	462	470 (FFT)	Quasi-ordered	159.9*	French Guiana, Brazil, arboreal
C. cyaneopubescens	Subadult, exuvia	Blue, leg	478	460 (FFT)	Quasi-ordered	141.1*	Venezuela, Paraguana, ground habitat
L. violaceopes	Adult, dissecting	Blue, leg	450	440 (FFT) 424 (ml)	Multilayer	Chitin: 92 ± 5 Air: 55 ± 6	Malaysia, Singapore, arboreal
E. cyanognathus	Spiderling, exuvia	Blue, chelicerae	458	440 (FFT) 388 (ml)	Multilayer[†]	Chitin: 76 ± 13[†] Air: 69 ± 12[†]	French Guiana, ground habitat
A. laeta	Spiderling, exuvia	Blue, leg	447.5	420 (FFT) 444 (ml)	Multilayer	Chitin: 86 ± 7 Air: 81 ± 8	Brazil, Puerto Rico, arboreal
P. metallica	Subadult, exuvia	Purple, leg	440	480 (FFT) 432 (ml)	Multilayer	Chitin: 83 ± 5 Air: 80 ± 5	India, arboreal
G. rosea	Adult, dissecting	Pink, carapace	459	n.a.	n.a.	n.a.	Chile, Bolivia, Argentina, ground habitat

*Calculated from predicted peak [½ × predicted peak (nm)/averaged refractive index]. †Based on Fig. 2E [TEM photo courtesy of R. F. Foelix (18)].

habitat for most blue tarantula species is the understory of tropical forests (Table 1). There, the ambient spectral composition of light is relatively consistent between day and night and is dominated by yellow-green with peak intensity at ~560 nm (44, 45). Many nocturnal animals have long wave–sensitive cone cell photoreceptors that match yellow-green wavelengths, thereby acting synergistically with the rod cells and enhancing their night vision (45). Thus, green colors may be rare in tarantulas simply because such colors would make them brighter and more conspicuous in the night to other species, including potential predators. Narrowband blue reflectance may therefore represent a compromise between being chromatically conspicuous to an unknown receiver (but not too bright) and becoming more difficult to be visually detected. Future work is needed to identify potential visual receiver species (for example, competitors and/or predators).

Structural color evolved differently in tarantulas under natural selection relative to lineages using colors in conspicuous mating displays evolving under sexual selection. In birds and insects, closely related species produce a variety of different colors through relatively rapid evolutionary changes in the periodic spatial distances of single types of nanostructure (25, 42). In tarantulas, similar colors are instead produced using different types of structural mechanisms, and those colors (especially blue) are conserved through long periods of evolutionary history and even across repeated origins of structural coloration. Tarantulas are thus a good model system to study structural color evolution under natural selection, bringing new perspectives and insights on our understanding of structural color evolution and possibly revealing new structural mechanisms or photonic nanostructure designs. For instance, the high angular independency found in the blue hairs of tarantulas (fig. S4) may inspire solutions to eliminate undesirable iridescent effects of structural color—a key factor limiting the use of structural colors in many human applications.

MATERIALS AND METHODS

Phylogeny and color survey
Phylogenetic relationships among 53 tarantula genera were resolved by constructing a supertree from previously published phylogenetic trees (37, 46–50). We performed a color survey by using digital images of tarantula species belonging to those 53 genera using Flickr and Google Image Search. Many images are available online because tarantulas are popular pets. However, surveyed images were taken from only two Web sites from experienced official sellers of tarantulas where taxonomic identification was assumed to be more accurate than that of general hobbyists. All species shown on their Web sites were considered in this study. Colors from distinct color patches in the images were sampled using the computer color picker (for example, the Mac OS X built-in DigitalColor Meter). Because the precise hue of any photo is determined in part by color balance settings of the camera and computer monitor, we binned colors into two broad categories: potential pigmentary colors (yellow, orange, red, brown, and black) and potential structural colors (blue, purple, magenta, green, and white) (fig. S2). We then mapped these data onto a phylogeny using genera as the operational taxonomic units, because of the unavailability of species-level phylogenetic relationships. Thus, a genus was considered "blue" even if only one species had the blue color. Color evolution was then reconstructed using Mesquite (Analysis:Tree → Trace Character Over Trees → Reconstruct Ancestral States → Stored Characters → Parsimony Ancestral States, http://mesquiteproject.org/) (Fig. 1).

Blue tarantulas
Tarantula specimens were purchased from private sellers. Eight species of tarantulas with blue color were arbitrarily selected on the basis of their photo descriptions and the availability on the trade market (fig. S2, boxes). Adult female L. violaceopes, G. rosea, and subadult E. pulcherrimaklaasi were purchased from http://tarantulaspiders.com. T. violaceus,

Hsiung et al. Sci. Adv. 2015;1:e1500709   27 November 2015

6 of 8

A. laeta, and *E. cyanognathus* spiderlings/subadults were purchased from Swift's Invertebrates. Subadult *C. cyaneopubescens* exuviae were purchased from Wild Things Inc. *P. metallica* exuvia was courteously made available by C. Desai (University of North Georgia, Dahlonega, GA) when on sabbatical in the Deheyn laboratory (University of California, San Diego–Scripps Institution of Oceanography).

Reflectance microspectrophotometry

Normally incident, specular reflectance spectra were measured across areas (4 × 4 µm) of the hairs using a 20/30 PV UV-Visible-NIR microspectrophotometer (CRAIC Technologies Inc.) (Fig. 2). Spectrum data across the human visible spectrum (350 to 750 nm) were collected using a 50× glass (ultraviolet-absorbent) objective lens. At least 15 measurements, each from a different hair of the same individual of each species, were collected. All spectra were then smoothened, aggregated, normalized, averaged, and analyzed using the R package "pavo" (*51*) using the following functions: getspec{pavo}; procspec(rspecdata, opt = c("smooth", "maximum", "minimum"), fixneg = c("zero")); aggplot{pavo} (http://cran.r-project.org/web/packages/pavo/index.html).

Electron microscopy

SEM analysis of tarantula hair morphology. Hairs (along with a small fragment of attached cuticle) were attached to SEM stubs using carbon tape, assisted with conductive silver paste when needed. Samples were sputter-coated with gold-palladium for 3 min under 20 mA and 1.4 kV and observed under SEM (JEOL 7401, Japan Electron Optics Laboratory Co. Ltd.) with 8-mm operating distance and 5-kV accelerating voltage.

TEM analysis of nanostructures within tarantula hair. Tarantula hairs and cuticle fragments were immersed in 0.25 M NaOH and 0.1% (v/v) Tween 20 solution for 30 min on a benchtop shaker. Samples were then transferred to formic acid/ethanol (2:3 v/v) solution and shaken for 2.5 hours. After that, the samples were washed with 100% ethanol and shaken for 20 min. Ethanol was replaced with fresh 100% ethanol and shaken for another 20 min. After two washes, the ethanol was replaced with fresh 100% ethanol for the last time, and the samples sat for another 24 hours to ensure complete dehydration. Epon resin infiltration was carried out in increasing Epon resin concentrations in acetone (15, 50, 70, and 100%). In each step, Epon resin was allowed to infiltrate for 24 hours. Samples were then placed in block molds and allowed to polymerize at 60°C for 16 hours. Epon resin consisted of 40% EMbed-812 (EMS #14120), 44% (soft)/32% (medium)/18% (hard) dodecenylsuccinic anhydride hardener (45346 FLUKA), 10% (soft)/16% (medium)/24% (hard) nadic methyl anhydride curing agent (00886-450, Polysciences Inc.), and ~2% promoter DMP-30 [2,4,6-tris(dimethylaminomethyl) phenol, SPI #02823-DA] or benzyl dimethylamine (AGR1062). The resulting polymerized blocks were trimmed using a Leica EM TRIM2 and cut into 80-nm sections using a diamond knife on an ultramicrotome (Leica EM UC6). Sections were mounted onto 100-mesh copper grids (EMS FCF100-Cu) and allowed to dry. Additional contrast-enhancer staining with uranyl acetate/lead citrate was performed as needed (see Uranyl Acetate/Lead Citrate Staining). The thickness of the observed chitin composite and air layers (Table 1) was measured from digital TEM micrographs using ImageJ.

Uranyl acetate/lead citrate staining

Grids were placed into the staining dish (PELCO 22510 Grid Staining Matrix System, Ted Pella Inc.). Then, the dish was dipped into the plastic holder containing 2% methanolic uranyl acetate (that is, 2% uranyl acetate dissolved in methanol) for 4 min and rinsed three times each with

methanol solution in decreasing concentrations (70, 50, and 30%). The dish was rinsed three more times with distilled water before it was dipped into Reynolds lead citrate solution (0.1% w/v lead citrate, 0.1 N NaOH, in distilled carbonate-free water) for 2 min. Then, the dish was rinsed five times with distilled water and sat on Kimwipes, and the grids were air-dried. Sections were then observed under TEM (JSM-1230, Japan Electron Optics Laboratory Co. Ltd.) at 120 kV.

Theoretical calculation

Coherent scattering model. We analyzed cross-sectional TEM micrographs in eight tarantula species, including *E. cyanognathus* [photo courtesy of R. F. Foelix (*18*)], using the Fourier Analysis Tool for Biological Nano-optics (*20*). This MATLAB-based program uses Fourier analysis to determine whether nanostructures are sufficiently organized at an appropriate scale to produce color by coherent light scattering. Quasi-ordered structures have a short-range (and not a long-range) order. FFT patterns (patterns that are shown in Fig. 3, column II) from anisotropic structures will vary depending on the directionality of the periodicity (Fig. 3, A to G, column II) and will be diffused if aperiodic (Fig. 3H, column II). Subsequent radial analyses incorporating the estimated n_r of the chitin composite of tarantula ($n_r = 1.63$) and air ($n_r = 1.00$) allow the user to obtain predicted reflectance spectra. Refractive indices used in the calculation are based on our index matching result (fig. S3). For all analyses, representative structural areas in TEM micrographs (Fig. 3, column I) were selected.

Multilayer model. We used a standard multilayer modeling in the R programming environment (*52*) to simulate the theoretical reflectance spectra for *L. violaceopes*, *E. cyanognathus*, *A. laeta*, and *P. metallica*, the four specimens that were observed to have conspicuous multilayer structures. The real n_r and extinction coefficient (k) of air ($n_r = 1.00$, $k = 0.00$) and the chitin composite ($n_r = 1.63$, $k = 0.06$) were used for the arithmetic calculation in the model based on published estimates (*53*) and the refractive index test (fig. S3). Three to four repeating units (a layer of chitin and a layer of air) on average were observed in micrographs of all four specimens excluding the cortex layer. Using three layers of the chitin composite and air each (three periodic repeats, six layers total) provided the best fit between theoretical and measured spectra.

SUPPLEMENTARY MATERIALS

REFERENCES AND NOTES

1. D. L. Fox, *Animal Biochromes and Structural Colours* (Univ. of California Press, Berkeley, CA, ed. 2, 1976).
2. M. D. Shawkey, G. E. Hill, Carotenoids need structural colours to shine. *Biol. Lett.* **1**, 121–124 (2005).
3. J. Sun, B. Bhushan, J. Tong, Structural coloration in nature. *RSC Adv.* **3**, 14862–14889 (2013).
4. J. A. Endler, Variation in the appearance of guppy color patterns to guppies and their predators under different visual conditions. *Vision Res.* **31**, 587–608 (1991).
5. C. L. Richards-Zawacki, M. E. Cummings, Intraspecific reproductive character displacement in a polymorphic poison dart frog, *Dendrobates pumilio*. *Evolution* **65**, 259–267 (2010).
6. P. R. Martin, R. Montgomerie, S. C. Lougheed, Color patterns of closely related bird species are more divergent at intermediate levels of breeding-range sympatry. *Am. Nat.* **185**, 443–451 (2015).
7. M. Irestedt, K. A. Jønsson, J. Fjeldså, L. Christidis, P. G. P. Ericson, An unexpectedly long history of sexual selection in birds-of-paradise. *BMC Evol. Biol.* **9**, 235 (2009).
8. H. B. Cott, *Adaptive Coloration in Animals* (Methuen & Co. Ltd., London, 1940).
9. T. Caro, The adaptive significance of coloration in mammals. *BioScience* **55**, 125–136 (2005).

10. H. K. Snyder, R. Maia, L. D'Alba, A. J. Shultz, K. M. C. Rowe, K. C. Rowe, M. D. Shawkey, Iridescent colour production in hairs of blind golden moles (Chrysochloridae). *Biol. Lett.* **8**, 393–396 (2012).

11. F. Barthelat, Nacre from mollusk shells: A model for high-performance structural materials. *Bioinspir. Biomim.* **5**, 035001 (2010).

12. V. Welch, J. P. Vigneron, V. Lousse, A. R. Parker, Optical properties of the iridescent organ of the comb-jellyfish *Beroë cucumis* (Ctenophora). *Phys. Rev. E* **73**, 041916 (2006).

13. N. A. Ayoub, C. Y. Hayashi, Spiders (Araneae), in *The Timetree of Life*, S. B. Hedges, S. Kumar, Eds. (Oxford Univ. Press, New York, 2009), pp. 255–259.

14. R. F. Foelix, *Biology of Spiders* (Oxford Univ. Press, New York, ed. 3, 2011).

15. W. Blein, K. Fauria, Y. Henaut, How does the tarantula *Lasiodora parahybana* Mello-Leitão, 1917 (Araneae, Theraphosidae) detects its prey? *Rev. Suisse Zool.* **1**, 71–78 (1996).

16. R. D. Dahl, A. M. Granda, Spectral sensitivities of photoreceptors in the ocelli of the tarantula *Aphonopelma chalcodes* (Araneae, Theraphosidae). *J. Arachnol.* **17**, 195–205 (1989).

17. P. Simonis, A. Bay, V. L. Welch, J.-F. Colomer, J. P. Vigneron, Cylindrical Bragg mirrors on leg segments of the male Bolivian blueleg tarantula *Pamphobeteus antinous* (Theraphosidae). *Opt. Express* **21**, 6979–6996 (2013).

18. R. F. Foelix, B. Erb, D. E. Hill, Structural colours in spiders, in *Spider Ecophysiology*, W. Nentwig, Ed. (Springer-Verlag, Berlin, Germany, 2013), pp. 333–347.

19. Z. Bálint, K. Kertész, G. Piszter, Z. Vértesy, L. P. Biró, The well-tuned blues: The role of structural colours as optical signals in the species recognition of a local butterfly fauna (Lepidoptera: Lycaenidae: Polyommatinae). *J. R. Soc. Interface* **9**, 1745–1756 (2012).

20. R. O. Prum, R. H. Torres, A Fourier tool for the analysis of coherent light scattering by bio-optical nanostructures. *Integr. Comp. Biol.* **43**, 591–602 (2003).

21. R. O. Prum, R. H. Torres, Fourier blues: Structural coloration of biological tissues, in *Excursions in Harmonic Analysis, Volume 2*, T. D. Andrews, R. Balan, J. J. Benedetto, W. Czaja, K. A. Okoudjou, Eds. (Birkhäuser Boston, Boston, MA, 2012), pp. 401–421.

22. R. Foelix, B. Rast, B. Erb, R. Thieleczek, Zur blauen und gelben Färbung von *Poecilotheria metallica* (Pocock, 1899). *Arachne* **17**, S4–S9 (2012).

23. P. Simonis, S. Berthier, How nature produces blue colors, in *Photonic Crystals—Introduction, Applications and Theory* (InTech, Rijeka, Croatia, 2012), pp. 1–22.

24. K. D. L. Umbers, On the perception, production and function of blue colouration in animals. *J. Zool.* **289**, 229–242 (2013).

25. M. Xiao, A. Dhinojwala, M. D. Shawkey, Nanostructural basis of rainbow-like iridescence in common bronzewing *Phaps chalcoptera* feathers. *Opt. Express* **22**, 14625–14636 (2014).

26. M. C. Stoddard, R. O. Prum, How colorful are birds? Evolution of the avian plumage color gamut. *Behav. Ecol.* **22**, 1042–1052 (2011).

27. S. M. Doucet, M. G. Meadows, Iridescence: A functional perspective. *J. R. Soc. Interface* **6** (Suppl. 2), S115–S132 (2009).

28. R. Maia, D. R. Rubenstein, M. D. Shawkey, Key ornamental innovations facilitate diversification in an avian radiation. *Proc. Natl. Acad. Sci. U.S.A.* **110**, 10687–10692 (2013).

29. M. F. Land, The morphology and optics of spider eyes, in *Neurobiology of Arachnids*, F. G. Barth, Ed. (Springer-Verlag, Berlin, Germany, 1985), pp. 53–76.

30. T. Nakamura, S. Yamashita, Learning and discrimination of colored papers in jumping spiders (Araneae, Salticidae). *J. Comp. Physiol. A* **186**, 897–901 (2000).

31. D. B. Zurek, T. W. Cronin, L. A. Taylor, K. Byrne, M. L. G. Sullivan, N. I. Morehouse, Spectral filtering enables trichromatic vision in colorful jumping spiders. *Curr. Biol.* **25**, R403–R404 (2015).

32. J. Defrize, C. E. Lazzari, E. J. Warrant, J. Casas, Spectral sensitivity of a colour changing spider. *J. Insect Physiol.* **57**, 508–513 (2011).

33. T. C. Insausti, J. Defrize, C. R. Lazzari, J. Casas, Visual fields and eye morphology support color vision in a color-changing crab-spider. *Arthropod Struct. Dev.* **41**, 155–163 (2012).

34. M. B. Girard, M. M. Kasumovic, D. O. Elias, Multi-modal courtship in the peacock spider, *Maratus volans* (O.P.-Cambridge, 1874). *PLOS One* **6**, e25390 (2011).

35. E. A. Hebets, Subadult experience influences adult mate choice in an arthropod: Exposed female wolf spiders prefer males of a familiar phenotype. *Proc. Natl. Acad. Sci. U.S.A.* **100**, 13390–13395 (2003).

36. E. A. Hebets, G. W. Uetz, Leg ornamentation and the efficacy of courtship display in four species of wolf spider (Araneae: Lycosidae). *Behav. Ecol. Sociobiol.* **47**, 280–286 (2000).

37. R. Bertani, Revision, cladistic analysis and biogeography of *Typhochlaena* C. L. Koch, 1850, *Pachistopelma* Pocock, 1901 and *Iridopelma* Pocock, 1901 (Araneae, Theraphosidae, Aviculariinae). *ZooKeys* **230**, 1–94 (2012).

38. N. E. Ferretti, A. A. Ferrero, Courtship and mating behavior of *Grammostola schulzei* (Schmidt 1994) (Araneae, Theraphosidae), a burrowing tarantula from Argentina. *J. Arachnol.* **36**, 480–483 (2008).

39. M. Heikkilä, L. Kaila, M. Mutanen, N. Peña, N. Wahlberg, Cretaceous origin and repeated tertiary diversification of the redefined butterflies. *Proc. Biol. Sci.* **279**, 1093–1099 (2012).

40. M. van Tuinen, Birds (Aves), in *The Timetree of Life*, S. B. Hedges, S. Kumar, Eds. (Oxford Univ. Press, New York, 2009), pp. 409–411.

41. M. Wiemers, B. V. Stradomsky, D. I. Vodolazhsky, A molecular phylogeny of *Polyommatus* s. str. and *Plebicula* based on mitochondrial *COI* and nuclear *ITS2* sequences (Lepidoptera: Lycaenidae). *Eur. J. Entomol.* **107**, 325–336 (2010).

42. B. R. Wasik, S. F. Liew, D. A. Lilien, A. J. Dinwiddie, H. Noh, H. Cao, A. Monteiro, Artificial selection for structural color on butterfly wings and comparison with natural evolution. *Proc. Natl. Acad. Sci. U.S.A.* **111**, 12109–12114 (2014).

43. A. Levy-Lior, E. Shimoni, O. Schwartz, E. Gavish-Regev, D. Oron, G. Oxford, S. Weiner, L. Addadi, Guanine-based biogenic photonic-crystal arrays in fish and spiders. *Adv. Funct. Mater.* **20**, 320–329 (2010).

44. J. A. Endler, The colour of light in forests and its implications. *Ecol. Monogr.* **63**, 1–27 (1993).

45. C. C. Veilleux, M. E. Cummings, Nocturnal light environments and species ecology: Implications for nocturnal color vision in forests. *J. Exp. Biol.* **215**, 4085–4096 (2012).

46. C. S. Fukushima, R. H. Nagahama, R. Bertani, The identity of *Mygale brunnipes* C.L. Koch 1842 (Araneae, Theraphosidae), with a redescription of the species and the description of a new genus. *J. Arachnol.* **36**, 402–410 (2008).

47. R. Bertani, R. H. Nagahama, C. S. Fukushima, Revalidation of *Pterinopelma* Pocock 1901 with description of a new species and the female of *Pterinopelma vitiosum* (Keyserling 1891) (Araneae: Theraphosidae: Theraphosinae). *Zootaxa* **2814**, 1–18 (2011).

48. R. C. West, S. C. Nunn, S. Hogg, A new tarantula genus, *Psednocnemis*, from West Malaysia (Araneae: Theraphosidae), with cladistic analyses and biogeography of Selenocosmiinae Simon 1889. *Zootaxa* **3299**, 1–43 (2012).

49. R. Bertani, J. P. L. Guadanucci, Morphology, evolution and usage of urticating setae by tarantulas (Araneae: Theraphosidae). *Zoologia* **30**, 403–418 (2013).

50. J. P. L. Guadanucci, Theraphosidae phylogeny: Relationships of the 'Ischnocolinae' genera (Araneae, Mygalomorphae). *Zool. Scr.* **43**, 508–518 (2014).

51. R. Maia, C. M. Eliason, P.-P. Bitton, S. M. Doucet, M. D. Shawkey, pavo: An R package for the analysis, visualization and organization of spectral data. *Methods Ecol. Evol.* **4**, 906–913 (2013).

52. R. Maia, J. V. O. Caetano, S. N. Báo, R. H. Macedo, Iridescent structural colour production in male blue-black grassquit feather barbules: The role of keratin and melanin. *J. R. Soc. Interface* **6** (Suppl. 2), S203–S211 (2009).

53. P. Vukusic, J. R. Sambles, C. R. Lawrence, R. J. Wootton, Quantified interference and diffraction in single *Morpho* butterfly scales. *Proc. Biol. Sci.* **266**, 1403 (1999).

54. S. Kinoshita, S. Yoshioka, Y. Fujii, N. Okamoto, Photophysics of structural color in the *Morpho* butterflies. *Forma* **17**, 103–121 (2002).

55. R. O. Prum, T. Quinn, R. H. Torres, Anatomically diverse butterfly scales all produce structural colours by coherent scattering. *J. Exp. Biol.* **209**, 748–765 (2006).

56. R. O. Prum, R. Torres, S. Williamson, J. Dyck, Two-dimensional Fourier analysis of the spongy medullary keratin of structurally coloured feather barbs. *Proc. Biol. Sci.* **266**, 13–22 (1999).

57. H. Yin, B. Dong, X. Liu, T. Zhan, L. Shi, J. Zi, E. Yablonovitch, Amorphous diamond-structured photonic crystal in the feather barbs of the scarlet macaw. *Proc. Natl. Acad. Sci. U.S.A.* **109**, 10798–10801 (2012).

58. E. Finger, D. Burkhardt, Biological aspects of bird colouration and avian colour vision including ultraviolet range. *Vision Res.* **34**, 1509–1514 (1994).

59. M. D. Shawkey, G. E. Hill, Significance of a basal melanin layer to production of non-iridescent structural plumage color: Evidence from an amelanotic Steller's jay (*Cyanocitta stelleri*). *J. Exp. Biol.* **209**, 1245–1250 (2006).

60. L. D'Alba, V. Saranathan, J. A. Clarke, J. A. Vinther, R. O. Prum, M. D. Shawkey, Colour-producing β-keratin nanofibres in blue penguin (*Eudyptula minor*) feathers. *Biol. Lett.* **7**, 543–546 (2011).

61. B. Ballentine, G. E. Hill, Female mate choice in relation to structural plumage coloration in blue grosbeaks. *Condor* **105**, 593–598 (2003).

62. M. D. Shawkey, S. L. Balenger, G. E. Hill, L. S. Johnson, A. J. Keyser, L. Siefferman, Mechanisms of evolutionary change in structural plumage coloration among bluebirds (*Sialia* spp.). *J. R. Soc. Interface* **3**, 527–532 (2006).

The following resources related to this article are available online at http://advances.sciencemag.org. (This information is current as of March 22, 2016):

Updated information and services, including high-resolution figures, can be found in the online version of this article at:
http://advances.sciencemag.org/content/1/10/e1500709.full

Supporting Online Material can be found at:
http://advances.sciencemag.org/content/suppl/2015/11/20/1.10.e1500709.DC1

This article **cites 53 articles,** 20 of which you can be accessed free:
http://advances.sciencemag.org/content/1/10/e1500709#BIBL